Supporting Information for

Peraurated Ruthenium Hydride Carbonyl Clusters: Aurophilicity, Isolobal Analogy, Structural Isomerism, and Fluxionality

Cristiana Cesari, Marco Bortoluzzi, Cristina Femoni, Francesca Forti, Maria Carmela Iapalucci, and Stefano Zacchini

[a] Dipartimento di Chimica Industriale "Toso Montanari", Università di Bologna, Viale Risorgimento 4 - 40136 Bologna. Italy.

[b] Dipartimento di Scienze Molecolari e Nanosistemi, Ca' Foscari University of Venice, Via Torino 155 – 30175 Mestre (Ve), Italy.

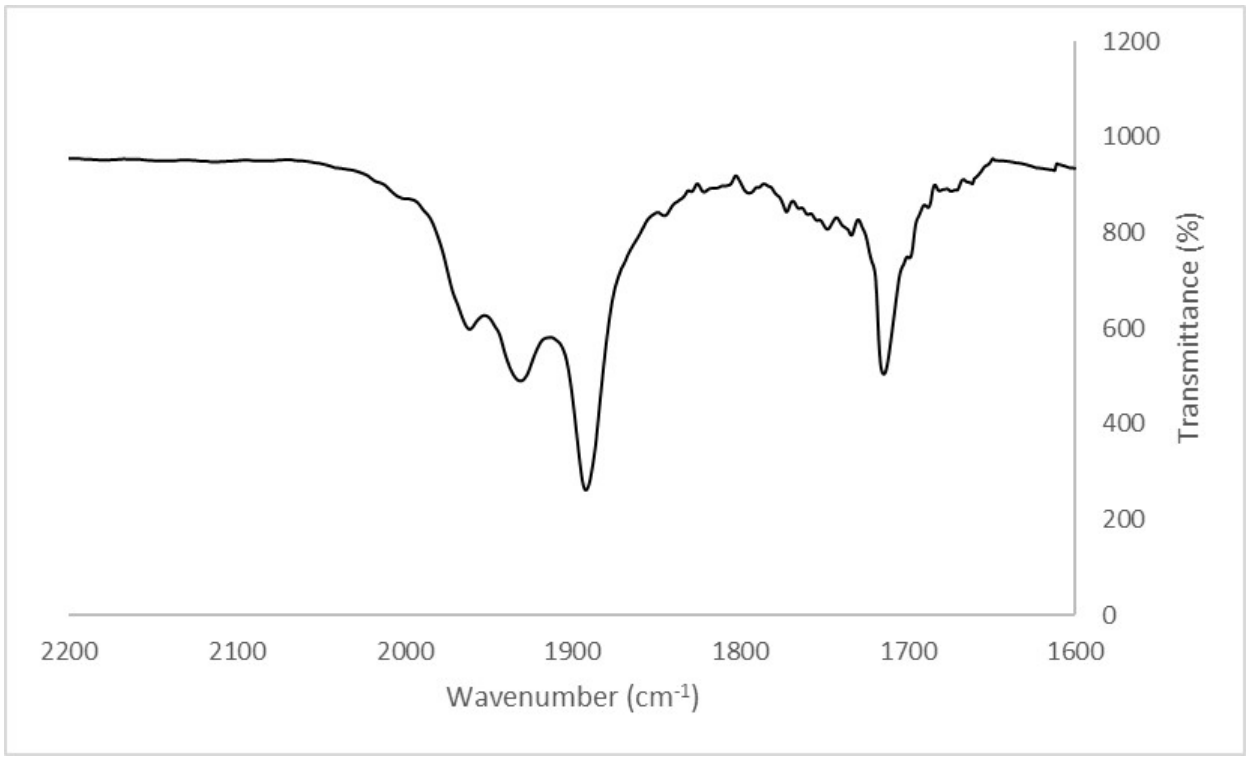

Figure S1. IR spectrum in the ν_{CO} region of $[NEt_4]_3[HRu_4(CO)_{12}]$ (**1**) in CH_3CN.

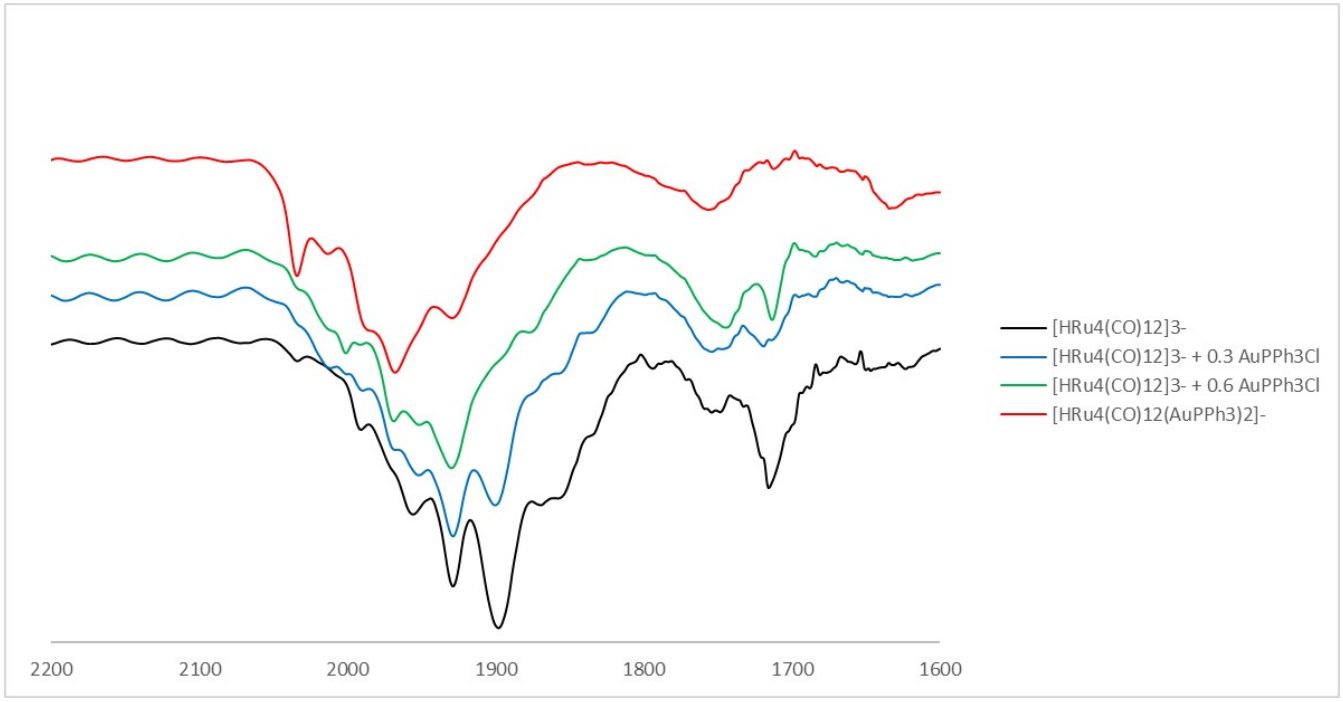

Figure S2. IR spectra of stepwise addition of $Au(PPh_3)Cl$ to a solution of $[NEt_4]_3[HRu_4(CO)_{12}]$ (**1**) in CH_3CN.

Figure S3. IR spectrum in the ν_{CO} region of $[NEt_4]_2[HRu_4(CO)_{12}(AuPPh_3)]$ (**2**) in CH_3CN.

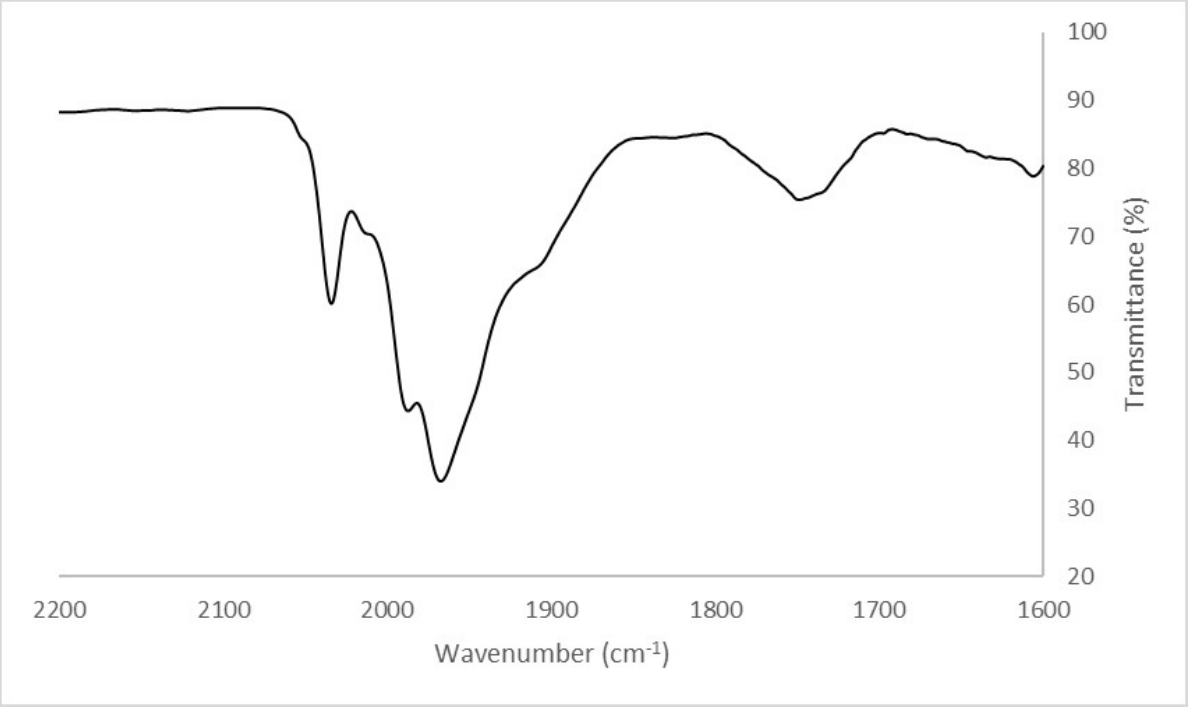

Figure S4. IR spectrum in the ν_{CO} region of $[NEt_4][HRu_4(CO)_{12}(AuPPh_3)_2]$ (**3**) in CH_2Cl_2.

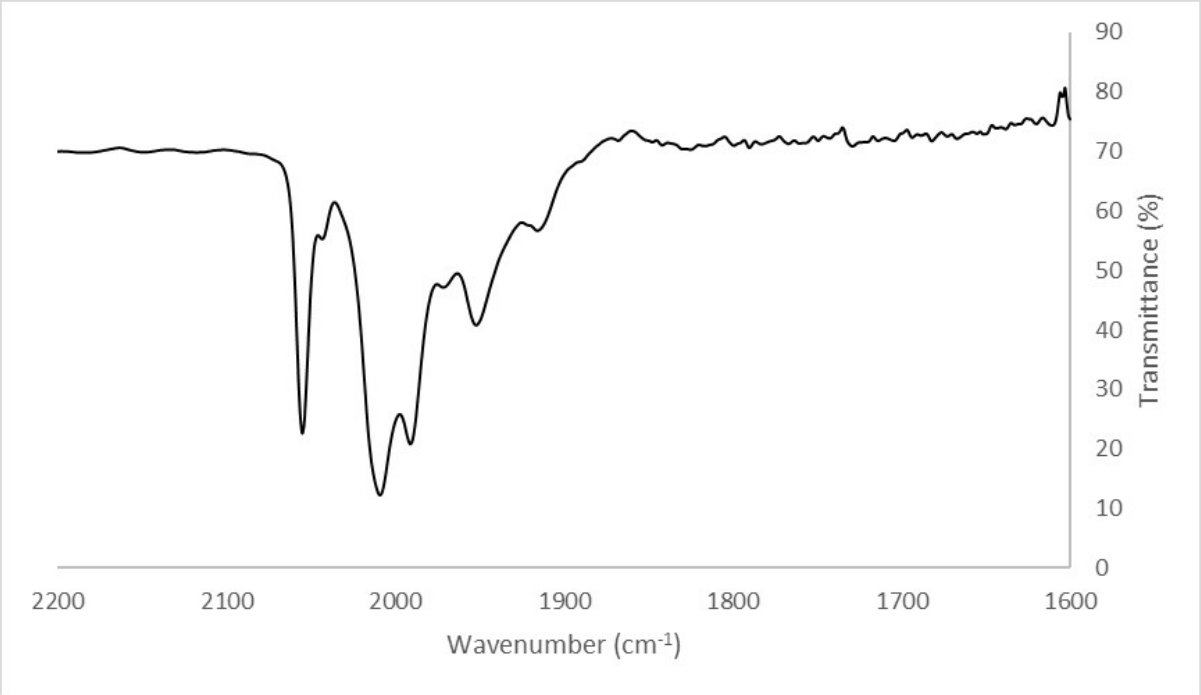

Figure S5. IR spectrum in the ν_{CO} region of $HRu_4(CO)_{12}(AuPPh_3)_3$ (**4**) in toluene.

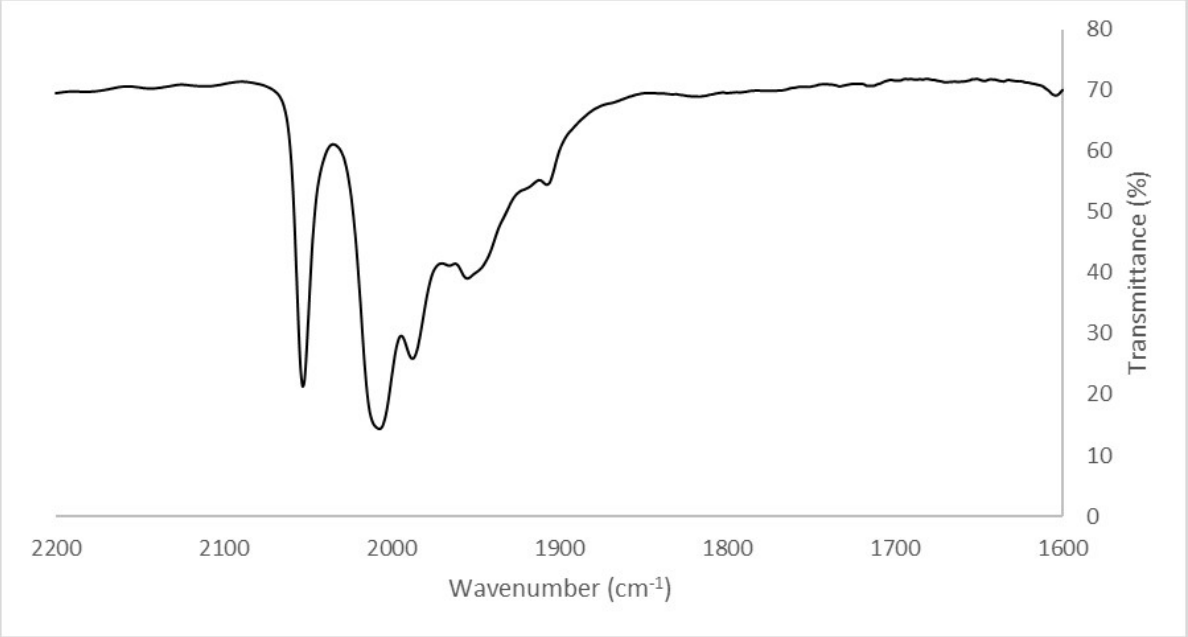

Figure S6. IR spectrum in the ν_{CO} region of $HRu_4(CO)_{12}(AuPPh_3)_3$ (**4**) in CH_2Cl_2.

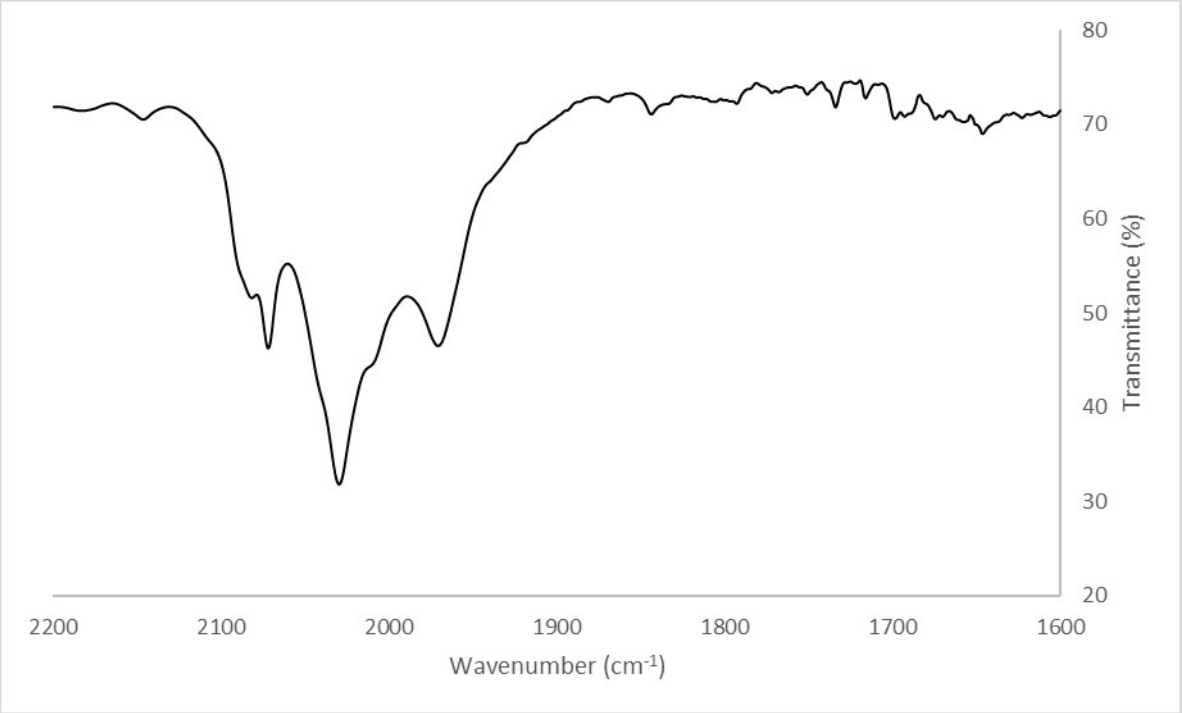

Figure S7. IR spectrum in the ν_{CO} region of $Ru_4(CO)_{12}(AuPPh_3)_4$ (**5**) in CH_2Cl_2.

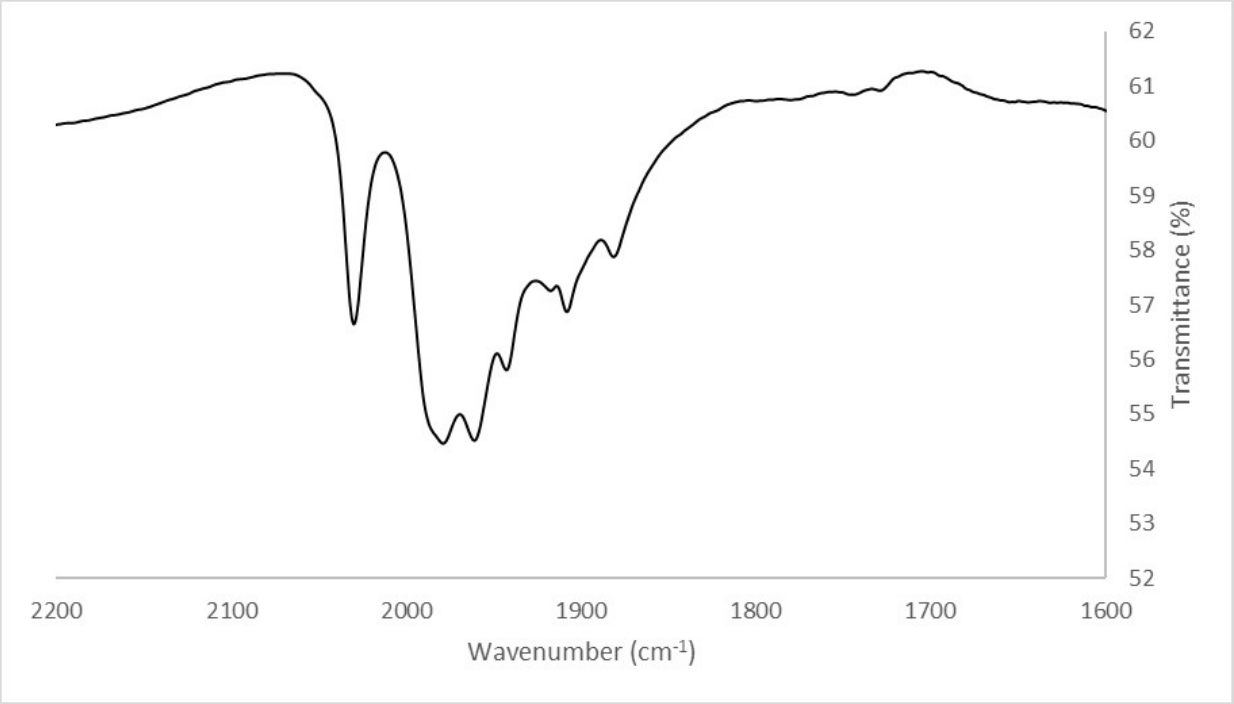

Figure S8. IR spectrum in the ν_{CO} region of $[NEt_4][HRu_4(CO)_{12}(AuPPh_3)_2]$ (**3**) in nujol mull.

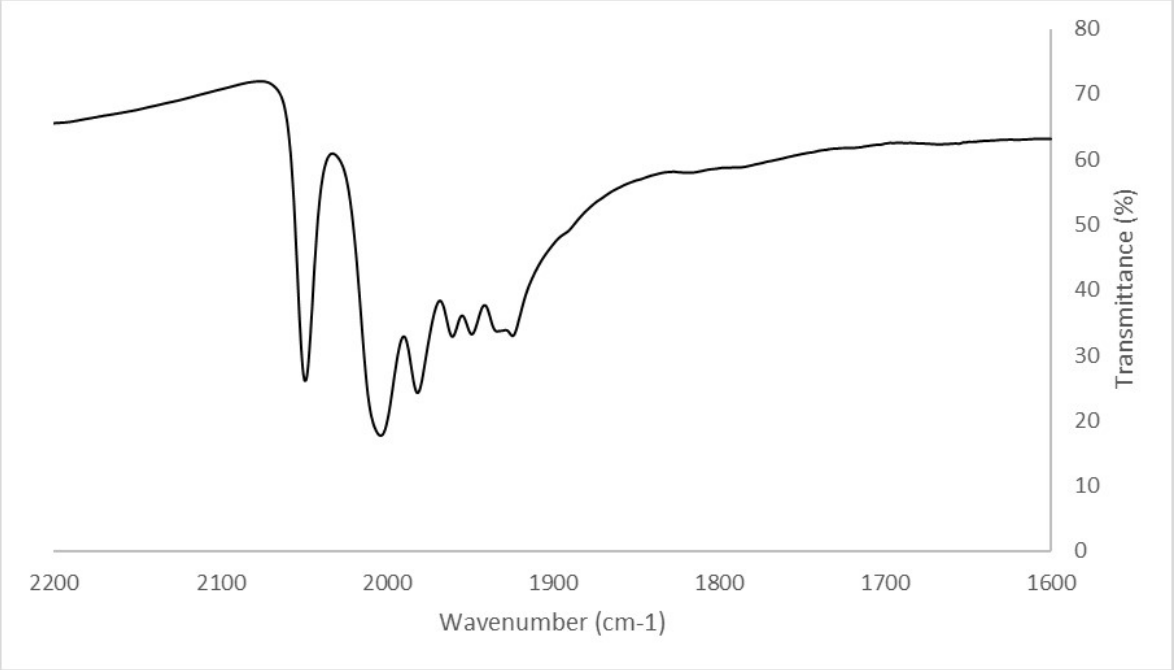

Figure S9. IR spectrum in the ν_{CO} region of $HRu_4(CO)_{12}(AuPPh_3)_3$ (**4**) in nujol mull.

Figure S10. IR spectrum in the ν_{CO} region of $Ru_4(CO)_{12}(AuPPh_3)_4$ (**5**) in nujol mull.

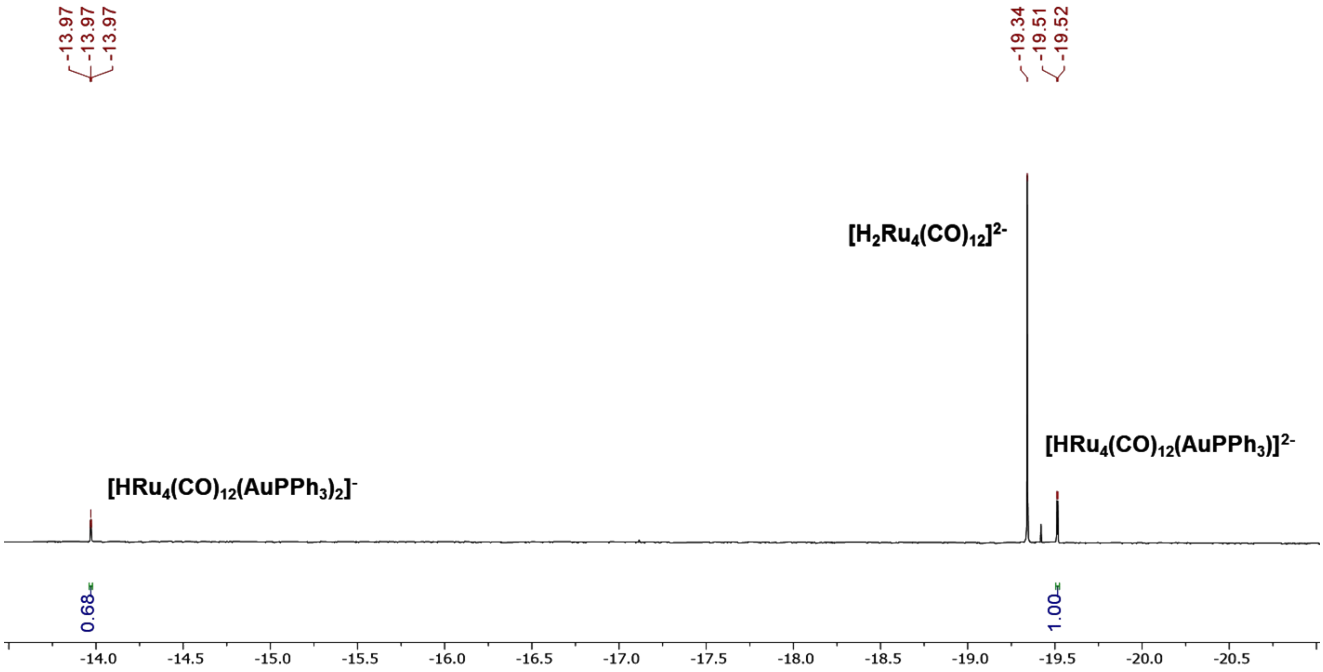

Figure S11. Hydride region of the ^{1}H NMR spectrum of mixture of $[H_2Ru_4(CO)_{12}]^{2-}$, $[HRu_4(CO)_{12}(AuPPh_3)_2]^{-}$ (**3**) and supposed $[HRu_4(CO)_{12}(AuPPh_3)]^{2-}$ (**2**) in CD_2Cl_2 at 298 K.

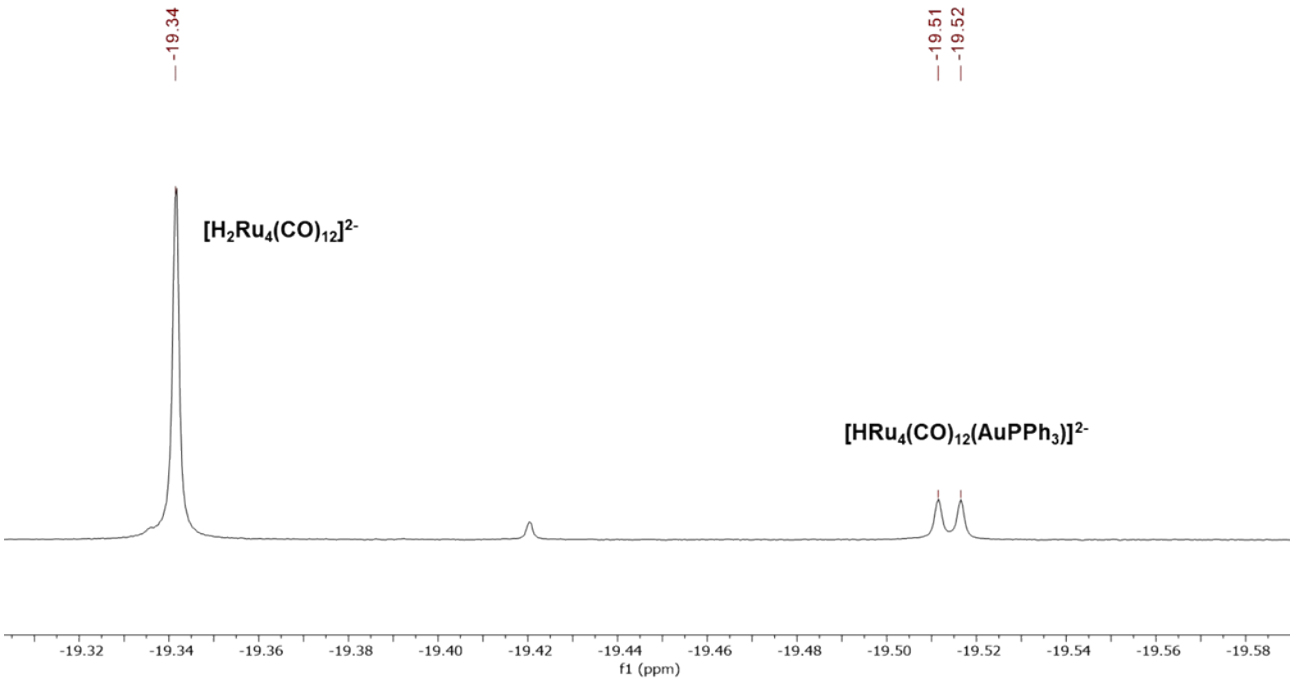

Figure S12. Hydride region of the ^{1}H NMR spectrum of mixture of $[H_2Ru_4(CO)_{12}]^{2-}$, $[HRu_4(CO)_{12}(AuPPh_3)_2]^{-}$ (**3**) and supposed $[HRu_4(CO)_{12}(AuPPh_3)]^{2-}$ (**2**) in CD_2Cl_2 at 298 K. Magnification of Figure S11.

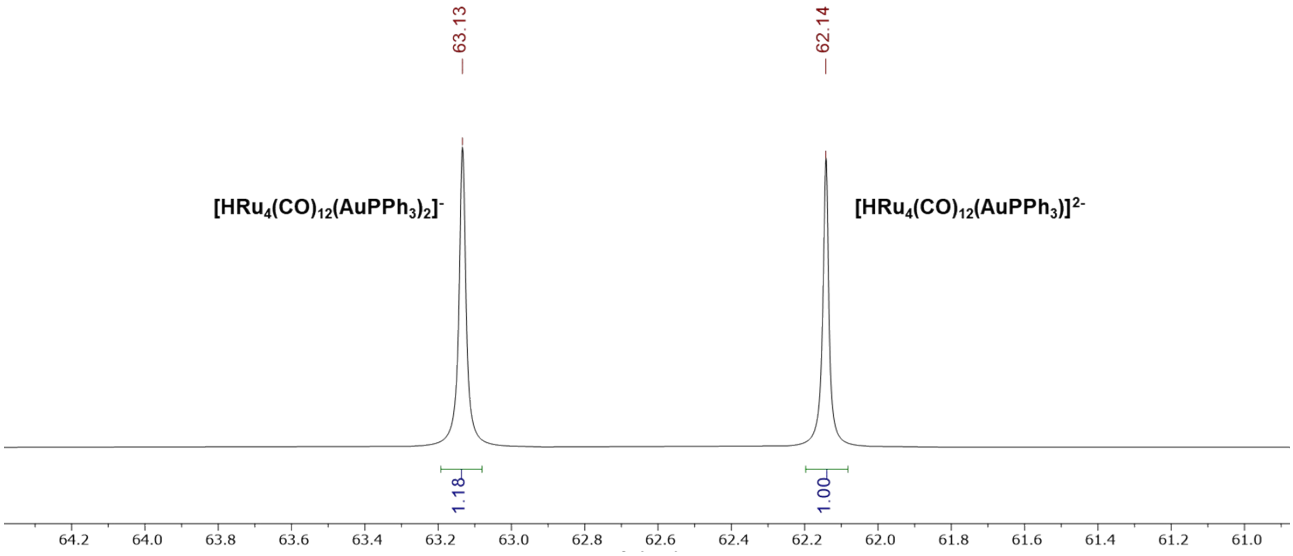

Figure S13. $^{31}P\{^{1}H\}$ NMR spectrum of mixture of $[HRu_4(CO)_{12}(AuPPh_3)_2]^-$ (**3**) and supposed $[HRu_4(CO)_{12}(AuPPh_3)]^{2-}$ (**2**) in CD_2Cl_2 at 298 K.

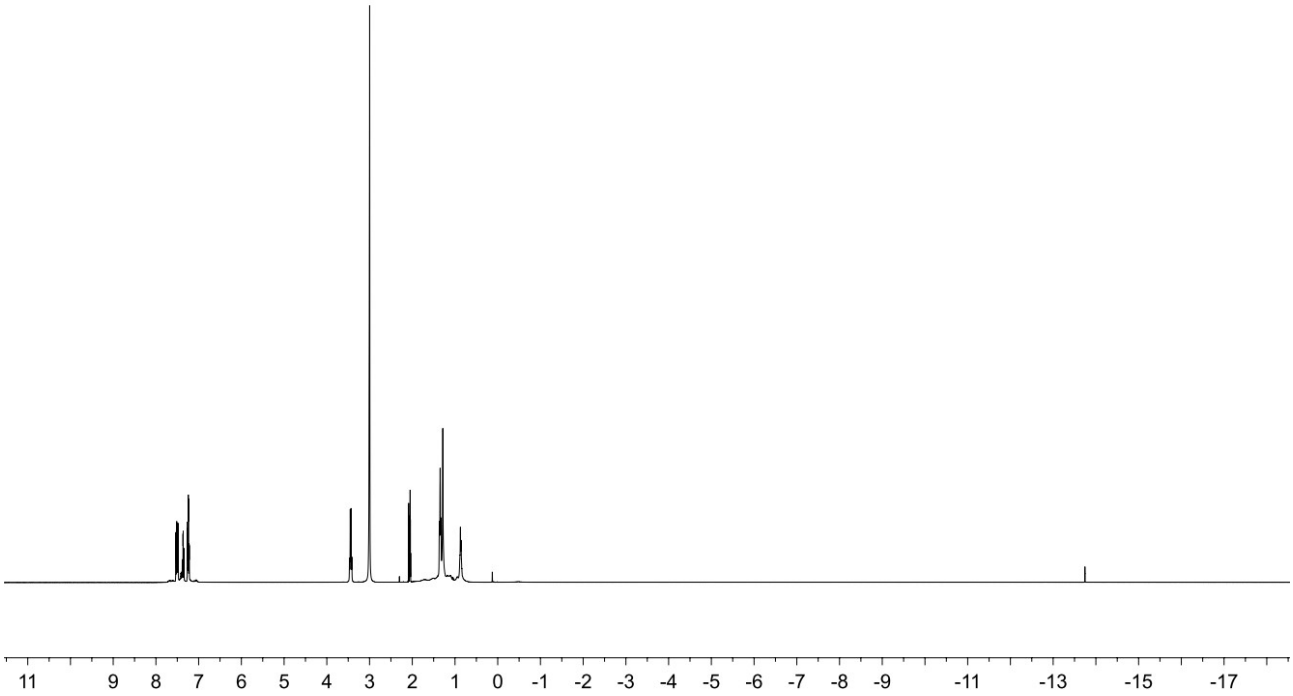

Figure S14. ^{1}H NMR spectrum of crystals of $[NEt_4][HRu_4(CO)_{12}(AuPPh_3)_2]$ (**3**) in acetone-d_6 at 298 K.

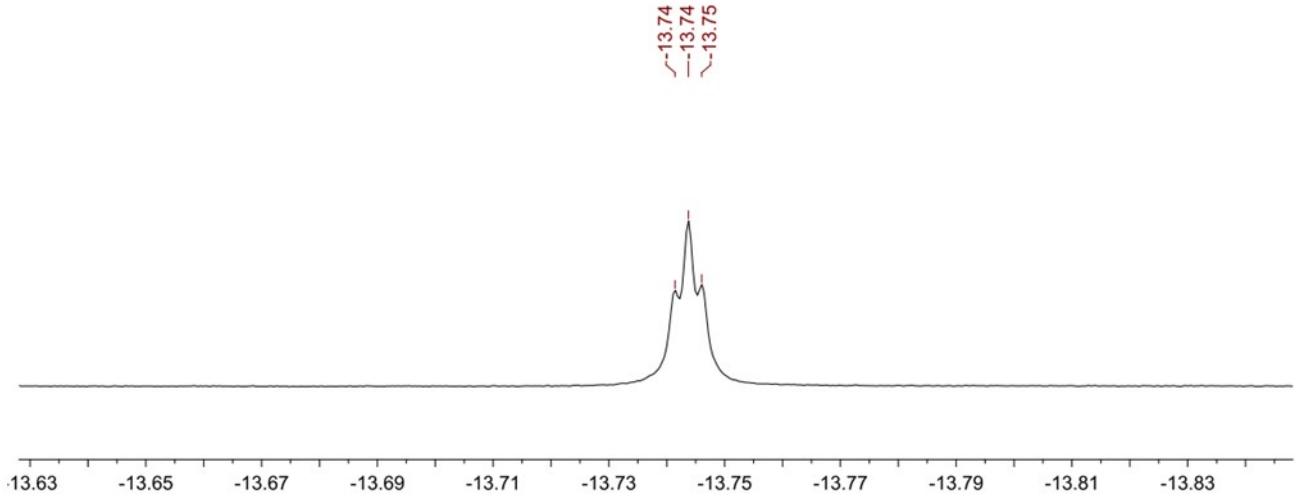

Figure S15. Hydride region of the ^{1}H NMR spectrum of $[NEt_4][HRu_4(CO)_{12}(AuPPh_3)_2]$ (**3**) in acetone-d_6 at 298 K.

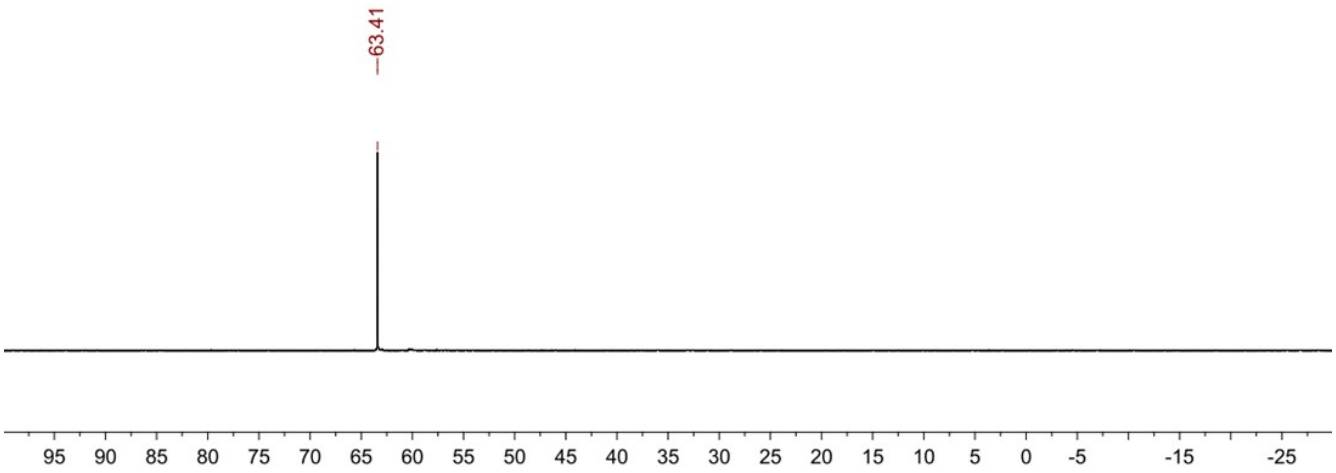

Figure S16. $^{31}P\{^{1}H\}$ NMR spectrum of $[NEt_4][HRu_4(CO)_{12}(AuPPh_3)_2]$ (**3**) in acetone-d_6 at 298 K.

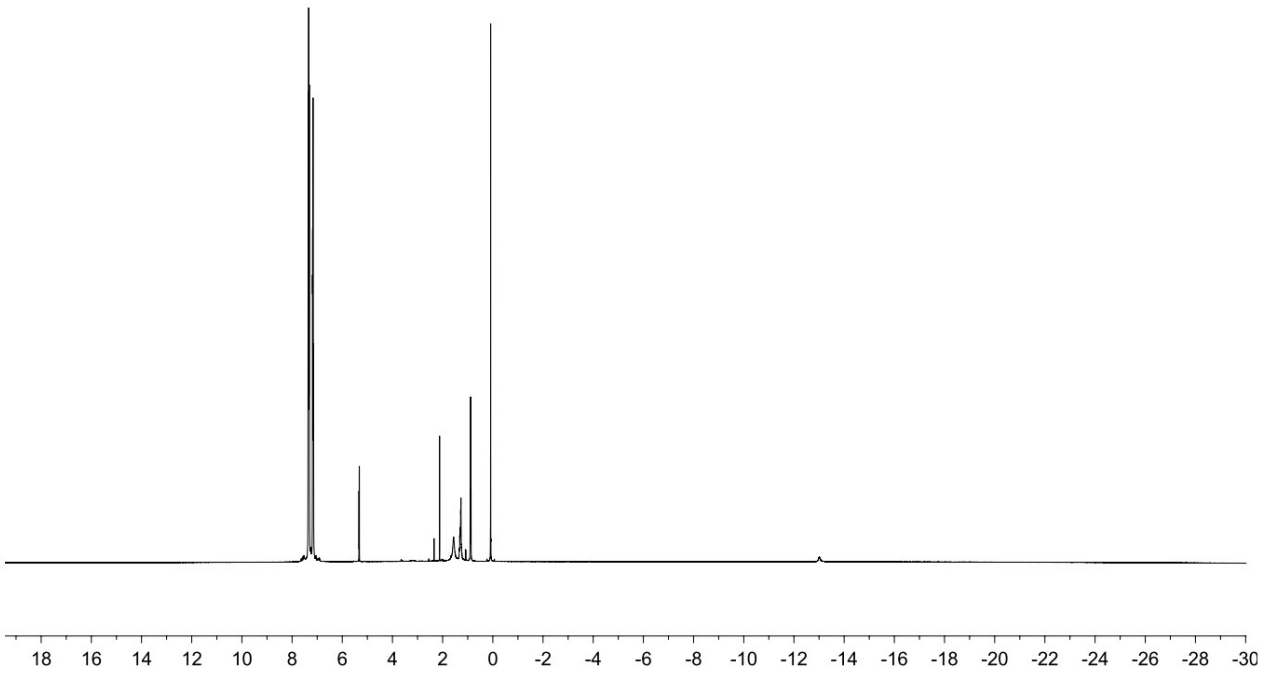

Figure S17. ^{1}H NMR spectrum of crystals of $HRu_4(CO)_{12}(AuPPh_3)_3$ (**4**) in CD_2Cl_2 at 298 K.

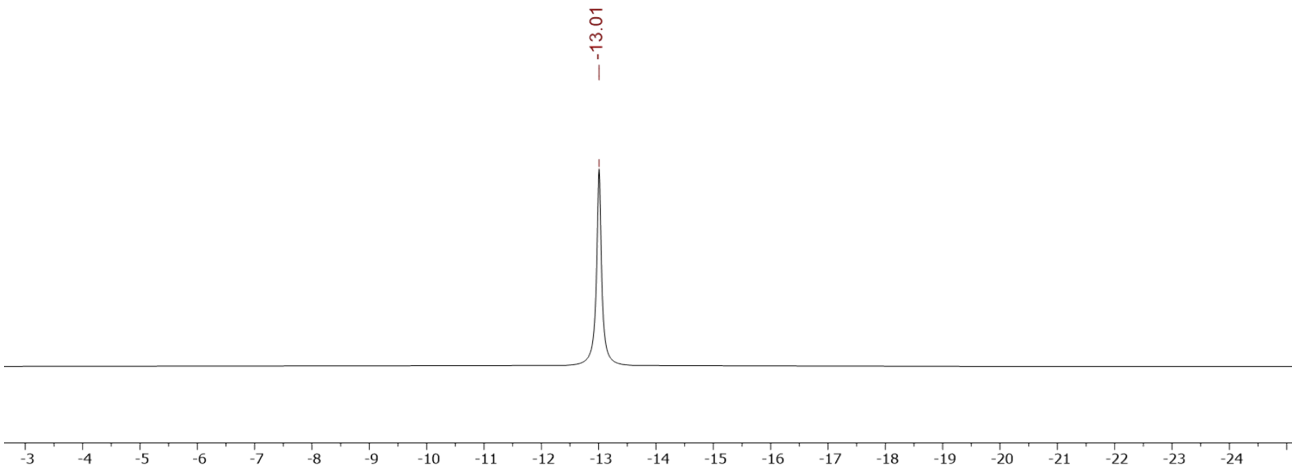

Figure S18. Hydride region of the ^{1}H NMR spectrum of crystals of $HRu_4(CO)_{12}(AuPPh_3)_3$ (**4**) in CD_2Cl_2 at 298 K.

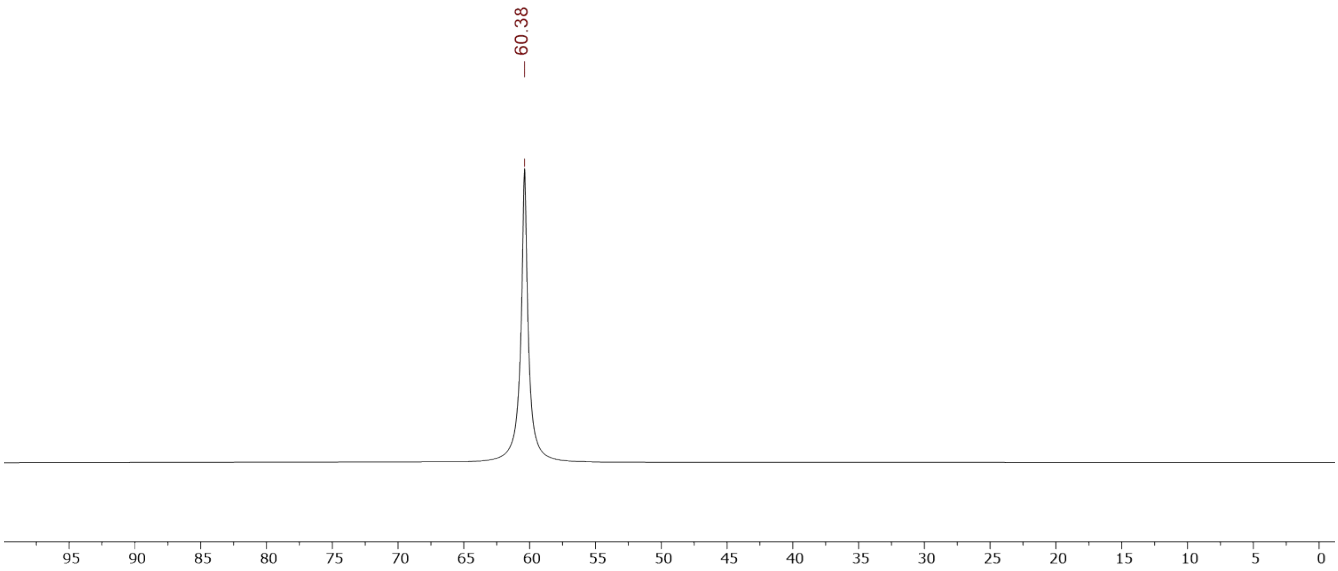

Figure S19. $^{31}P\{^{1}H\}$ NMR spectrum of crystals of $HRu_4(CO)_{12}(AuPPh_3)_3$ (**4**) in CD_2Cl_2 at 298 K.

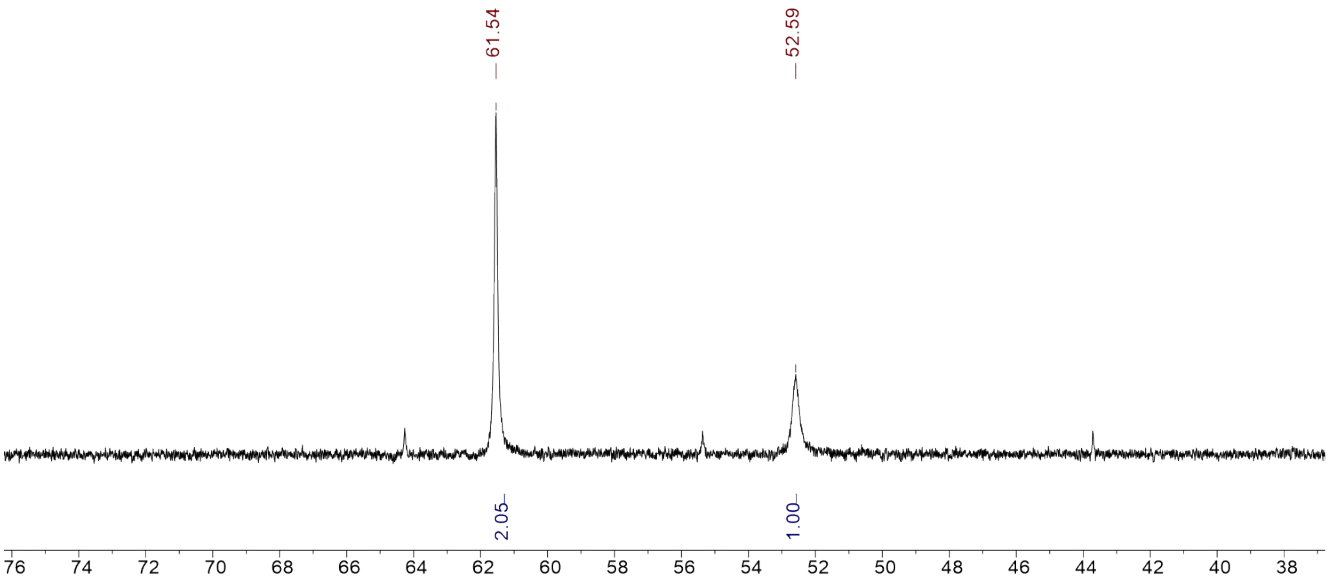

Figure S20. $^{31}P\{^{1}H\}$ NMR spectrum of crystals of $HRu_4(CO)_{12}(AuPPh_3)_3$ (**4**) in CD_2Cl_2 at 248 K.

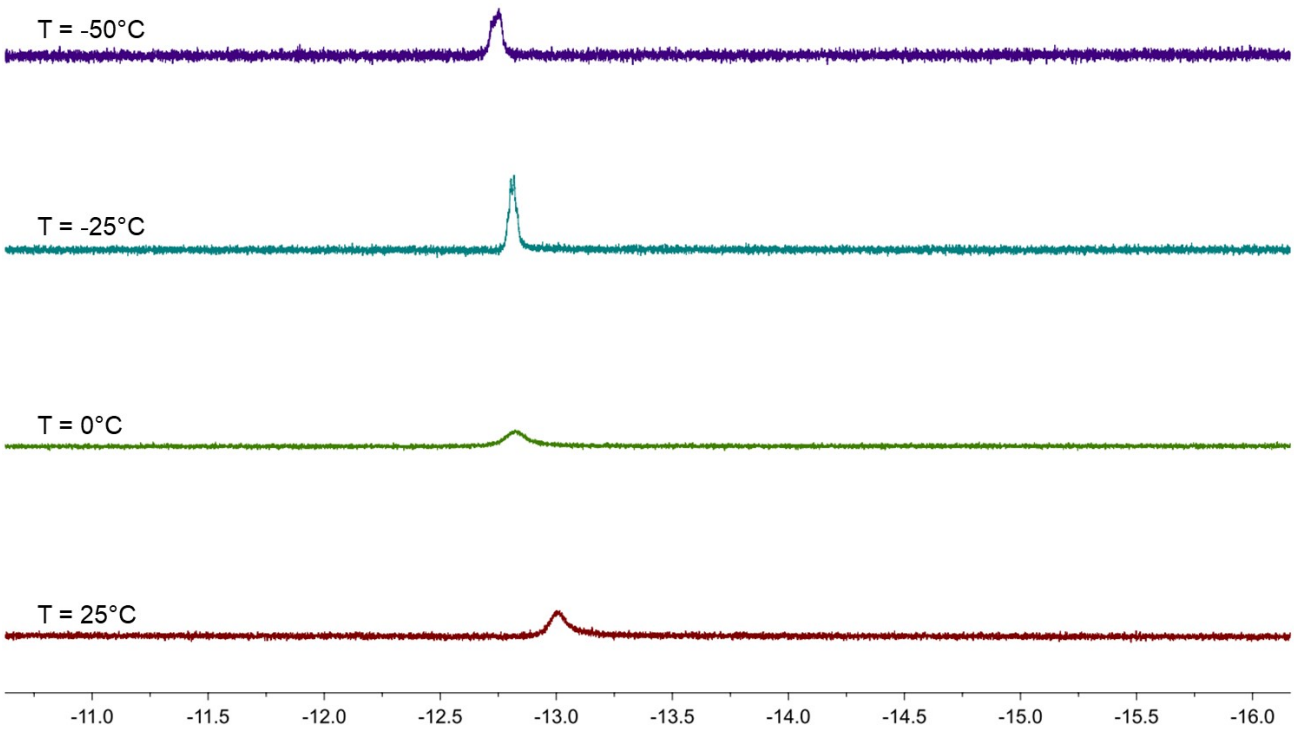

Figure S21. Hydride region of the VT ^{1}H NMR spectra of $HRu_4(CO)_{12}(AuPPh_3)_3$ (**4**) in CD_2Cl_2 (400 MHz).

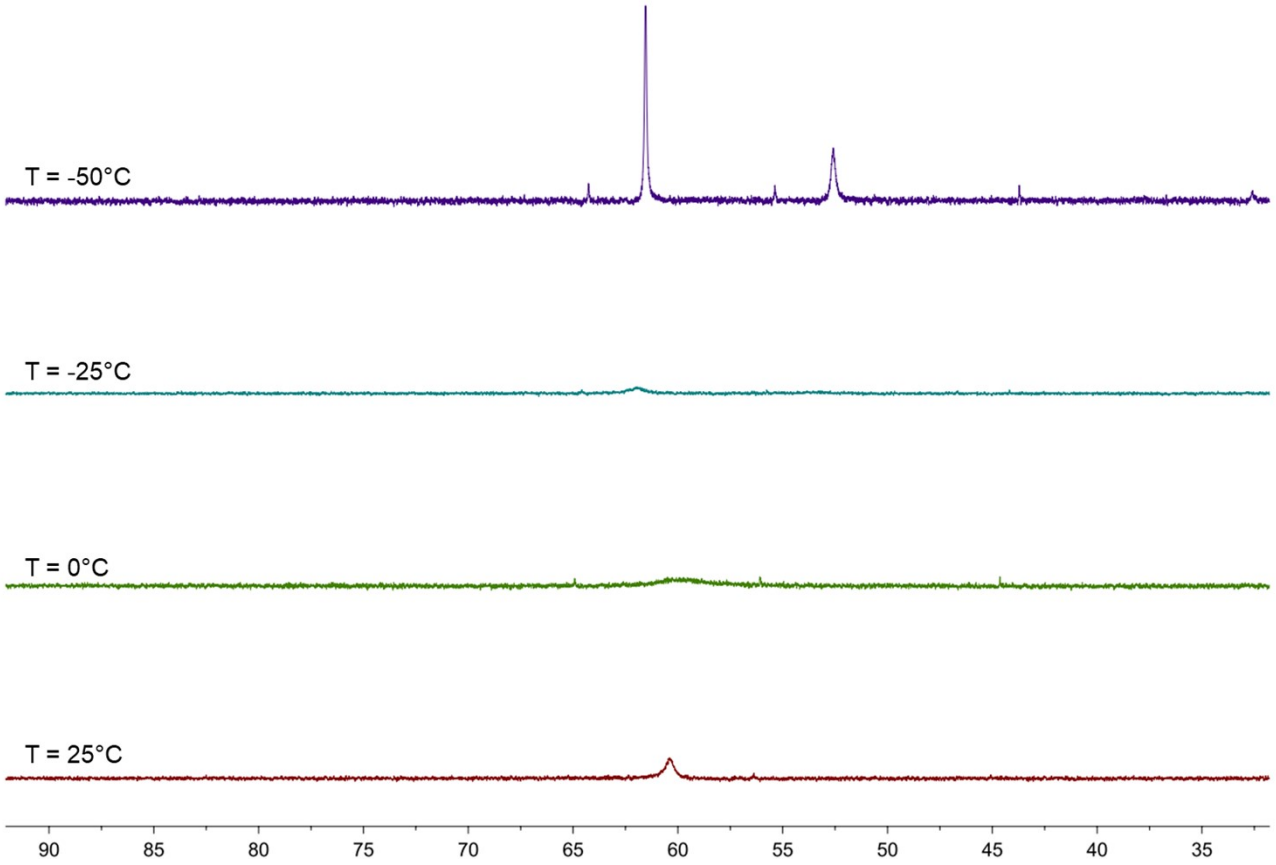

Figure S22. VT $^{31}P\{^{1}H\}$ NMR spectra of $HRu_4(CO)_{12}(AuPPh_3)_3$ (**4**) in CD_2Cl_2 (400 MHz).

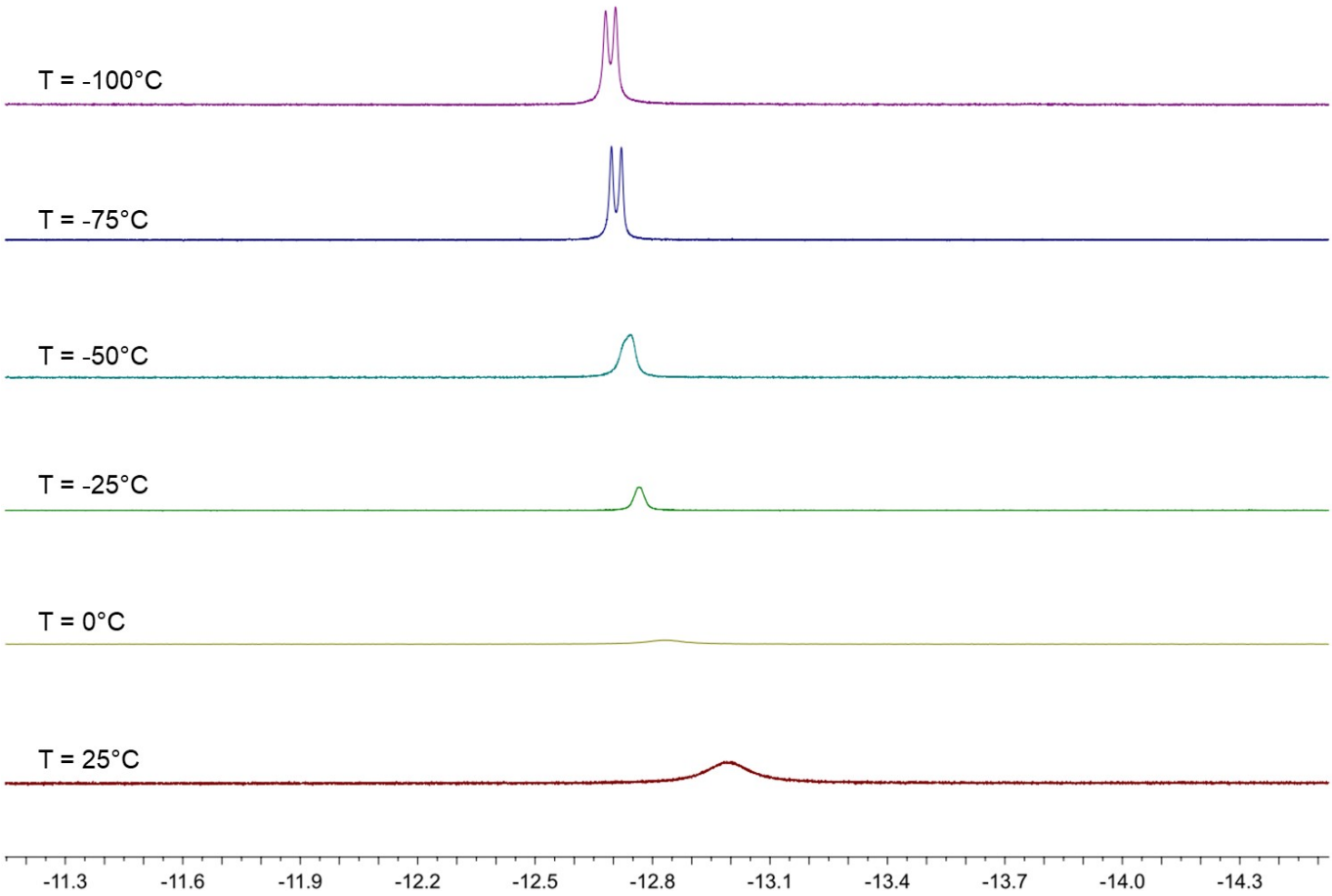

Figure S23. Hydride region of the VT ^{1}H NMR spectra of $HRu_4(CO)_{12}(AuPPh_3)_3$ (**4**) in CD_2Cl_2 (600 MHz).

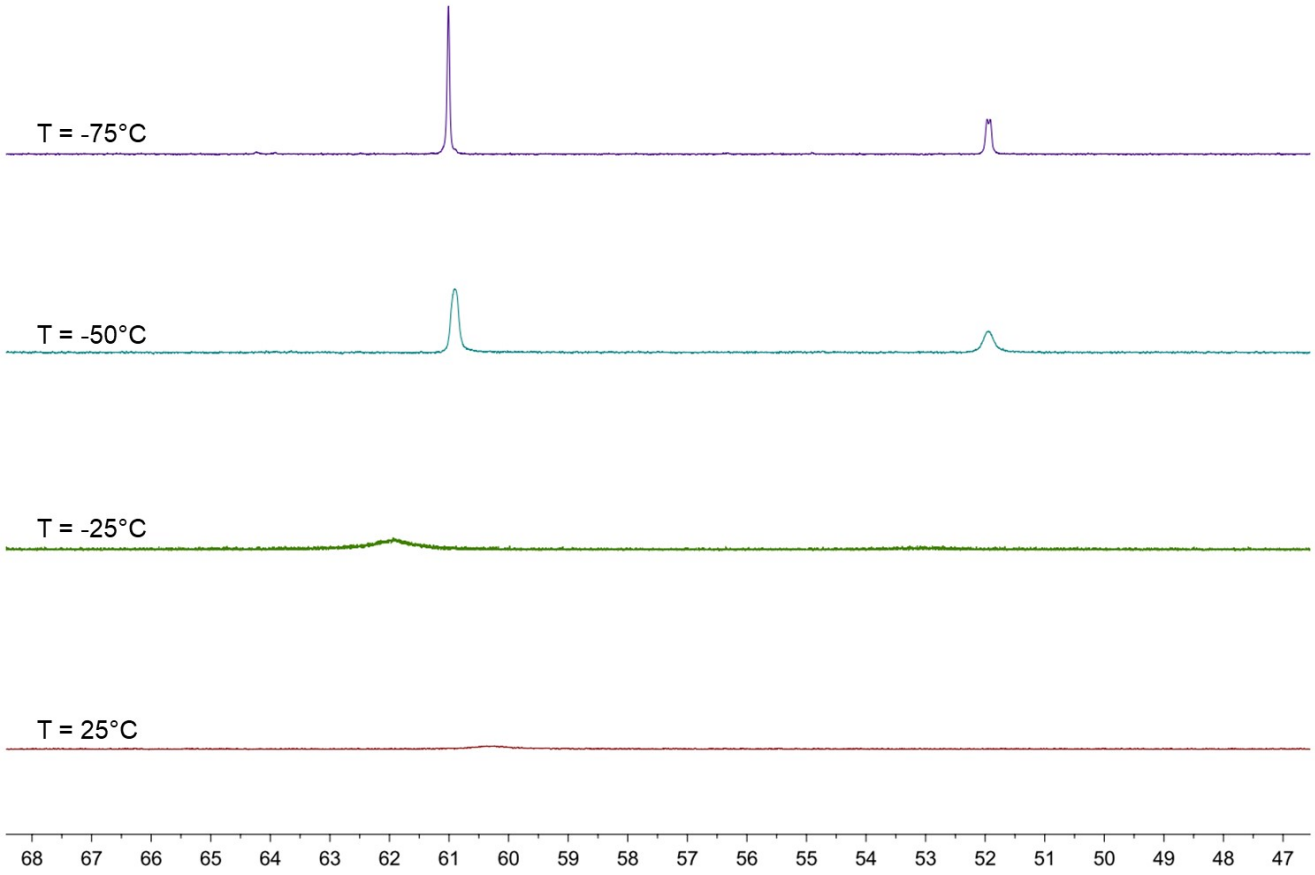

Figure S24. VT $^{31}P\{^{1}H\}$ NMR spectra of $HRu_4(CO)_{12}(AuPPh_3)_3$ (**4**) in CD_2Cl_2 (600 MHz).

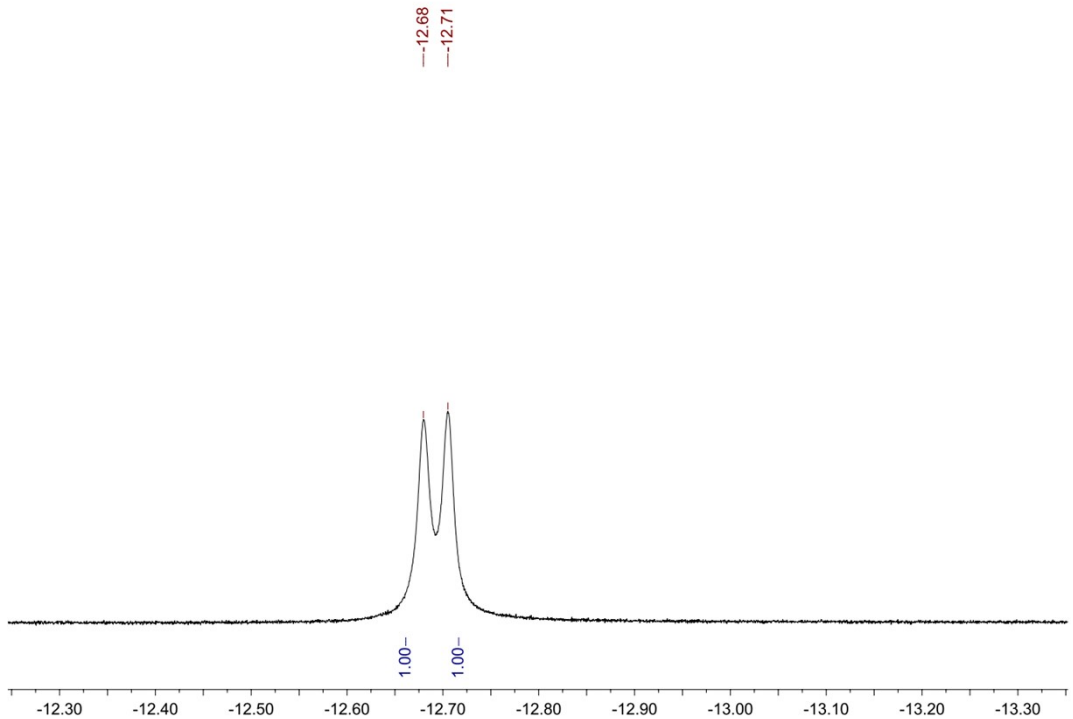

Figure S25. Hydride region of the ^{1}H NMR spectrum of $HRu_4(CO)_{12}(AuPPh_3)_3$ (**4**) in CD_2Cl_2 at 173K (600 MHz).

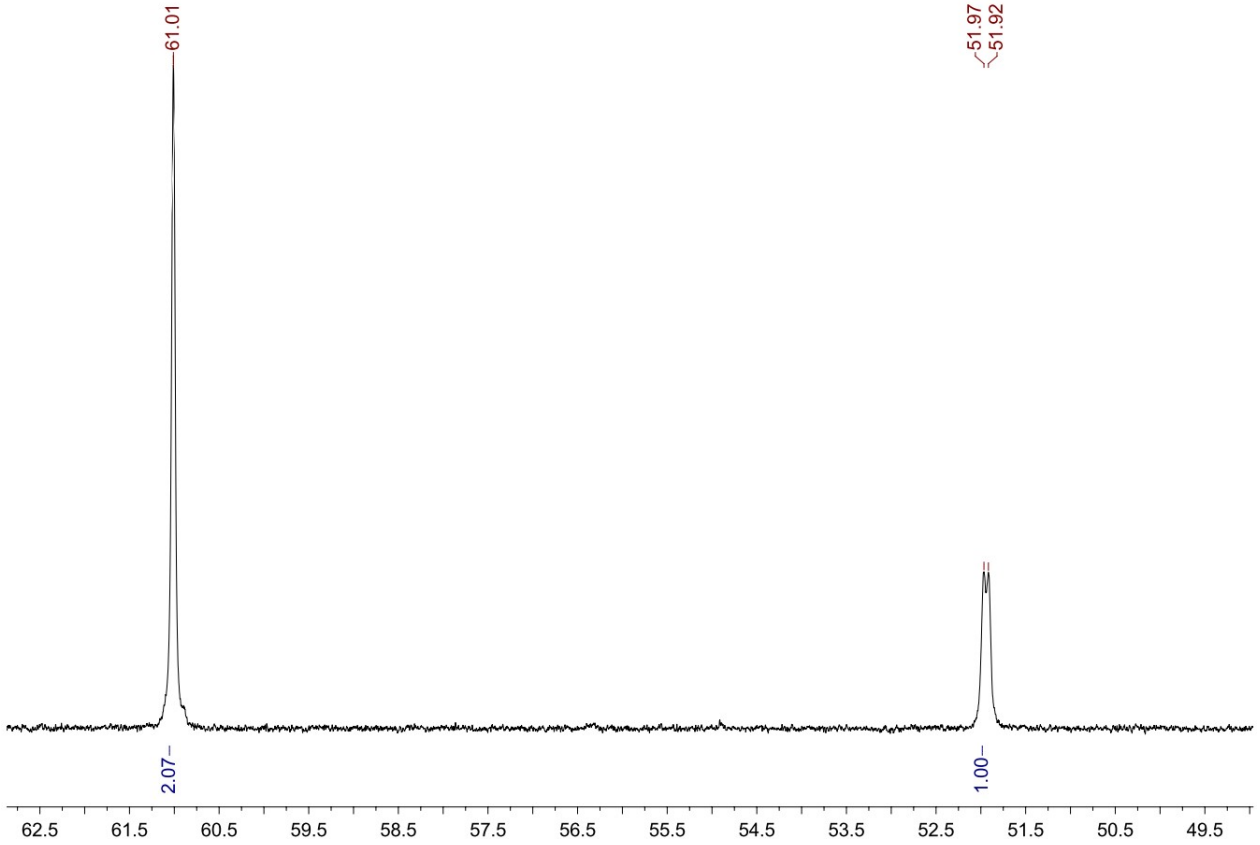

Figure S26. $^{31}P\{^{1}H\}$ NMR spectrum of $HRu_4(CO)_{12}(AuPPh_3)_3$ (**4**) in CD_2Cl_2 at 198 K (600 MHz).

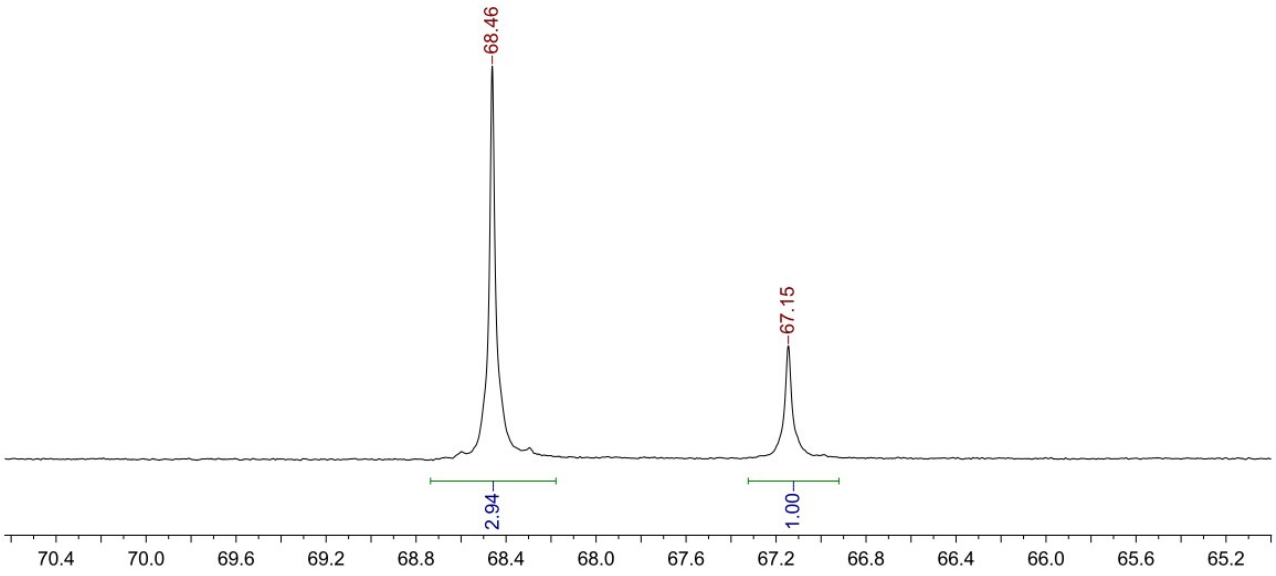

Figure S27. $^{31}P\{^{1}H\}$ NMR spectrum of $Ru_4(CO)_{12}(AuPPh_3)_4$ (**5**) in CD_2Cl_2 at 298 K.

Table S1.

Crystal data and experimental details for $[NEt_4][\mathbf{3}]\cdot 2CH_2Cl_2$, **4-b**$\cdot 2CH_2Cl_2$, **4-a**, **5**$\cdot 0.5CH_2Cl_2\cdot$solv, and **5**$\cdot$solv.

	$[NEt_4][3]\cdot 2CH_2Cl_2$	**4-b$\cdot 2CH_2Cl_2$**	**4-a**
Formula	$C_{58}H_{55}Au_2Cl_4NO_{12}P_2Ru_4$	$C_{68}H_{50}Au_3Cl_4O_{12}P_3Ru_4$	$C_{66}H_{46}Au_3O_{12}P_3Ru_4$
Fw	1959.98	2288.97	2119.11
T, K	100(2)	100(2)	100(2)
λ, Å	0.71073	0.71073	0.71073
Crystal system	Triclinic	Monoclinic	Triclinic
Space Group	$P\bar{1}$	$P2_1/n$	$P\bar{1}$
a, Å	14.5146(8)	13.8772(12)	13.2702(19)
b, Å	14.8691(8)	21.705(2)	14.563(2)
c, Å	15.0629(9)	23.920(2)	18.762(3)
α, °	90.759(2)	90	108.410(4)
β, °	95.483(2)	96.818(3)	98.613(4)
γ, °	96.132(2)	90	109.110(4)
Cell Volume, Å^3	3216.6(3)	7153.7(11)	3118.3(8)
Z	2	4	2
D_c, g cm^{-3}	2.024	2.125	2.257
μ, mm^{-1}	5.733	7.225	8.111
F(000)	1876	4320	1992
Crystal size, mm	0.19×0.15×0.12	0.22×0.18×0.14	0.15×0.11×0.07
θ limits, °	1.866–25.999	1.618-27.000	1.608-25.010
Index ranges	-17 ≤ h ≤ 17 -18 ≤ k ≤ 18 -18 ≤ l ≤ 18	-17 ≤ h ≤ 17 -27 ≤ k ≤ 27 -30 ≤ l ≤ 30	-15 ≤ h ≤ 15 -17 ≤ k ≤ 17 -22 ≤ l ≤ 22
Reflections collected	42391	98857	31342
Independent reflections	12625 [R_{int} = 0.0490]	15372 [R_{int} = 0.0459]	10940 [R_{int} = 0.0816]
Completeness to θ max	99.9%	99.5%	98.4%
Data / restraints / parameters	12625 / 1 / 755	15372 / 86 / 860	10940 / 495 / 688

Goodness on fit on F^2	1.071	1.204	1.136
R_1 ($I > 2\sigma(I)$)	0.0346	0.0328	0.0820
wR_2 (all data)	0.0808	0.0689	0.1891
Largest diff. peak and hole, e $Å^{-3}$	2.636 / –1.149	1.417 / -1.485	3.419 / -4.098

	5·0.5CH_2Cl_2·solv	**5·solv**
Formula	$C_{84.5}H_{61}Au_4ClO_{12}P_4Ru_4$	$C_{84}H_{60}Au_4O_{12}P_4Ru_4$
Fw	2619.81	2577.34
T, K	100(2)	100(2)
λ, Å	0.71073	0.71073
Crystal system	Monoclinic	Monoclinic
Space Group	*C*2/*c*	$P2_1/c$
a, Å	24.253(2)	21.680(12)
b, Å	14.1328(12)	15.264(9)
c, Å	50.610(4)	28.645(17)
α, °	90	90
β, °	95.833(3)	92.504(15)
γ, °	90	90
Cell Volume, $Å^3$	17258(3)	9473(9)
Z	8	4
D_c, g cm^{-3}	2.017	1.807
μ, mm^{-1}	7.615	6.908
F(000)	9864	4848
Crystal size, mm	0.21×0.14×0.08	0.15×0.14×0.10
θ limits, °	1.670-25.049	1.512-25.000
Index ranges	-28 ≤ h ≤ 28 -16 ≤ k ≤ 16 -60 ≤ l ≤ 60	-25 ≤ h ≤ 25 -18 ≤ k ≤ 18 -34 ≤ l ≤ 31
Reflections collected	103921	51811
Independent reflections	15231 [R_{int} = 0.0757]	16593 [R_{int} = 0.0902]
Completeness	99.6%	99.4%

to θ max		
Data / restraints / parameters	15231 / 708 / 835	16593 / 438 / 973
Goodness on fit on F^2	1.140	1.041
R_1 ($I > 2\sigma(I)$)	0.0771	0.0683
wR_2 (all data)	0.1689	0.1826
Largest diff. peak and hole, e $Å^{-3}$	3.530 / –5.878	3.251 / –2.325

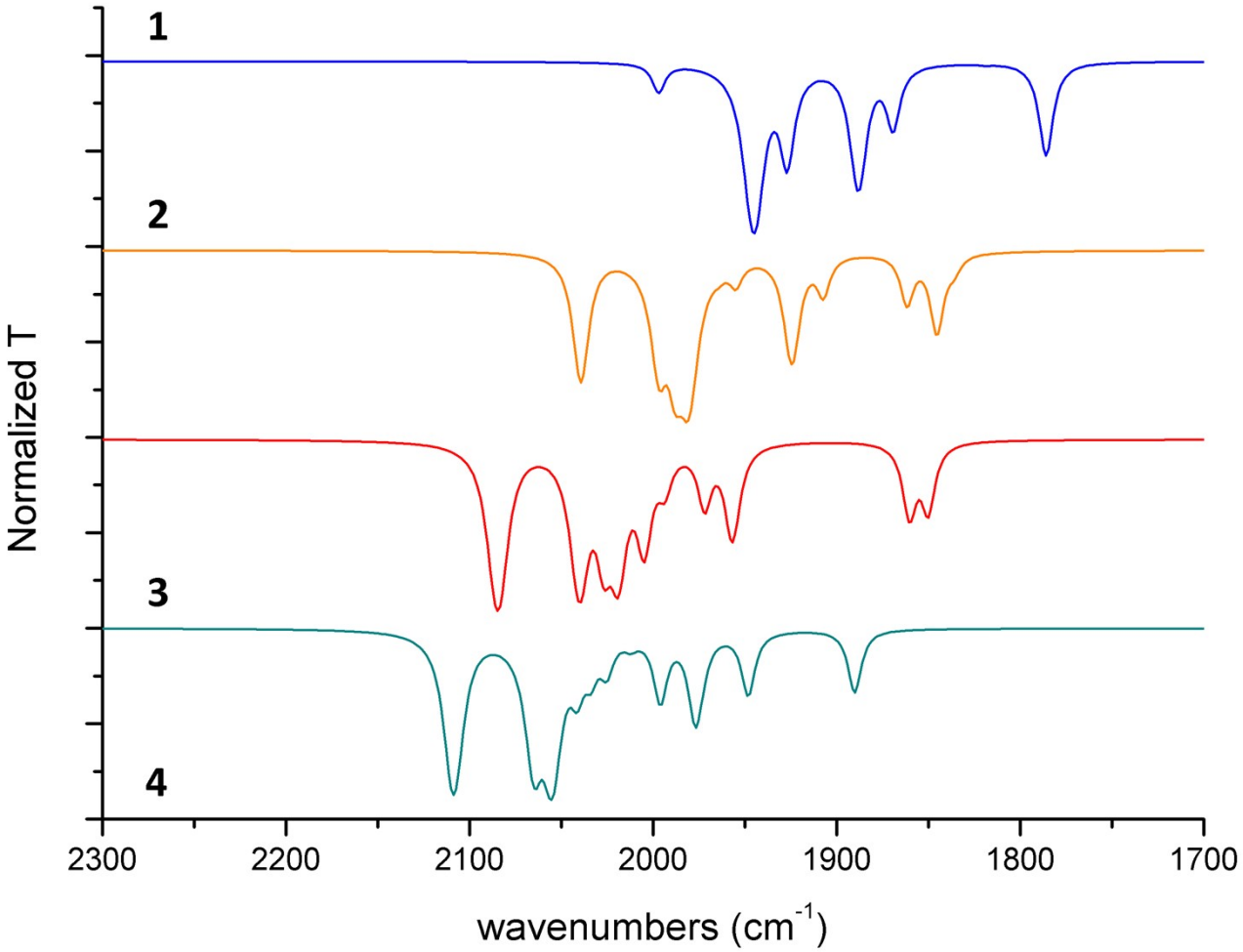

Figure S28. Simulated IR spectra (Lorentzian broadening functions, FWHM = 8 cm^{-1}). The **4-b** isomer is reported for compound **4**.

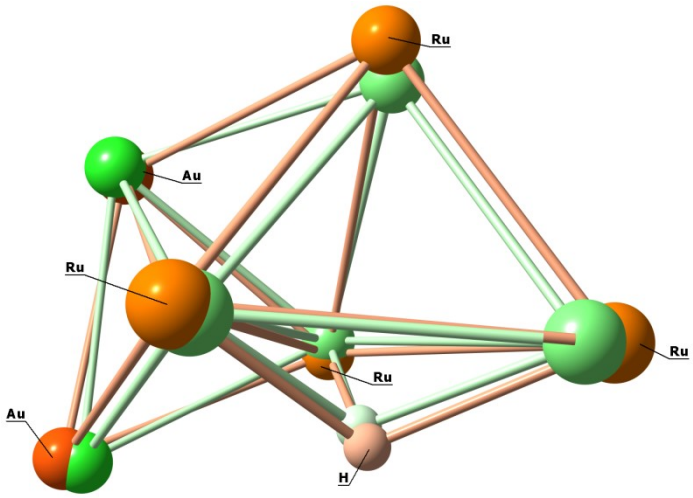

Figure S29. Best superposition of the DFT-optimized HM_4Au_2 fragments (M = Ru, Fe) in **3** and $[HFe_4(CO)_{12}(AuPPh_3)_2]^-$. M = Ru, orange tones; M = Fe, green tones.

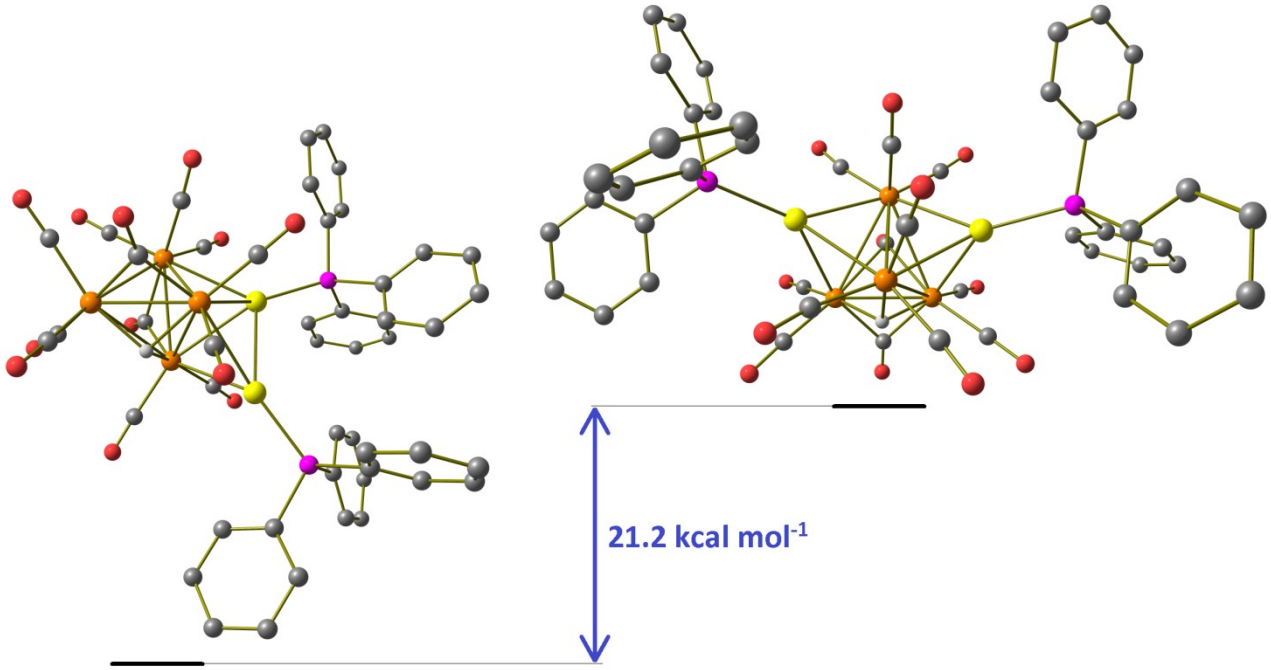

Figure S30. DFT-optimized geometry of **3** and of a possible symmetric isomer with Gibbs energy difference (orange Ru; yellow Au; purple P; red O; grey C; white H; hydrogen atoms on the phenyl rings omitted for clarity).

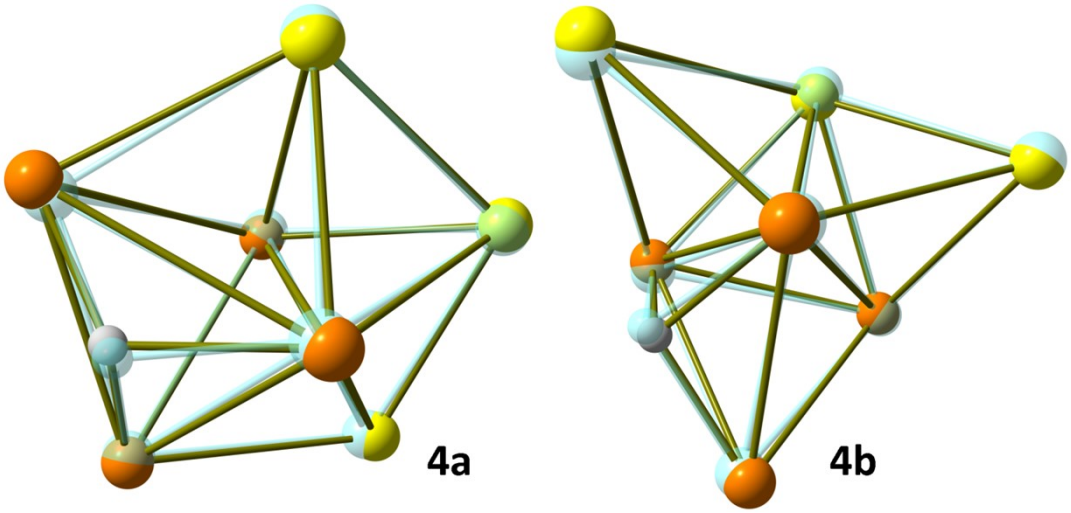

Figure S31. Best superpositions of the DFT-optimized HRu_4Au_3 fragments of **4-a** and **4-b** (orange Ru; yellow Au; white H) with the X-Ray data (transparent cyan).

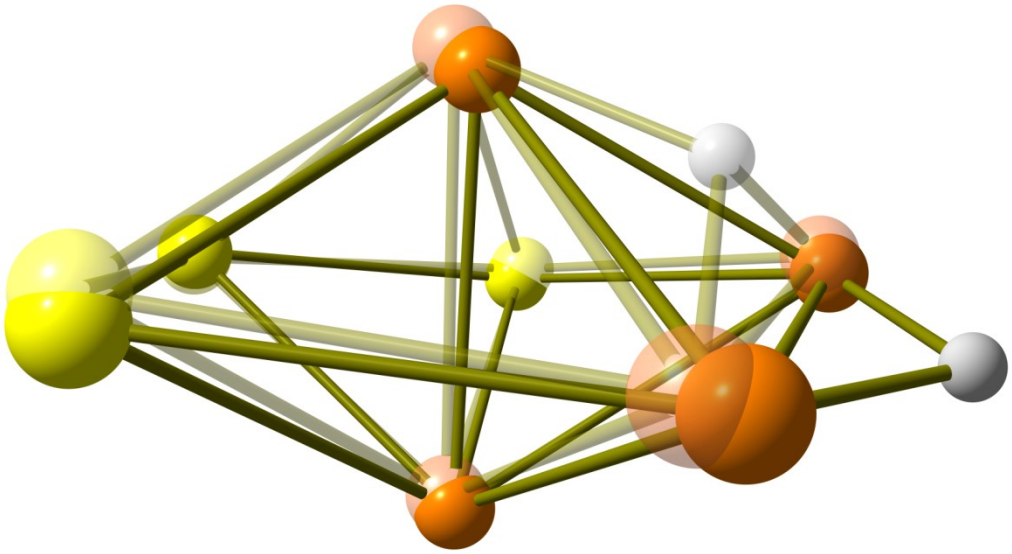

Figure S32. Best superpositions of the DFT-optimized HRu_4Au_3 fragments of **4-a** (orange Ru; yellow Au; white H) in gas phase (transparent) and in the presence of DMSO as implicit solvent (solid).

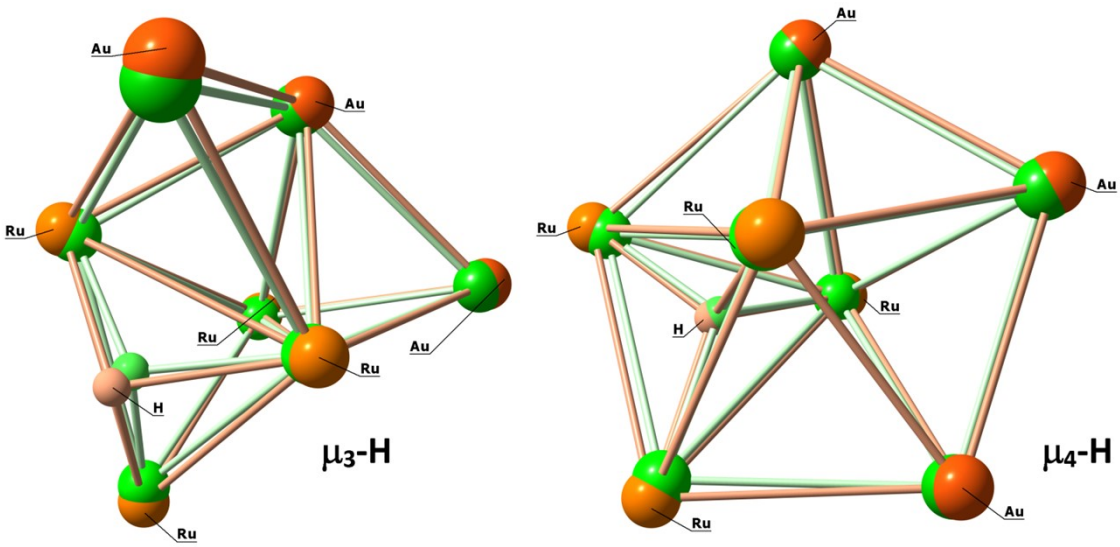

Figure S33. Best superpositions of the DFT-optimized fragments HRu_4Au_3 (orange tones) and HFe_4Au_3 (green tones) in **4-b** and its Fe analogue (**μ_3-H**) and between the Ru and Fe isomers with the hydride inside the Ru_4 cage (**μ_4-H**).

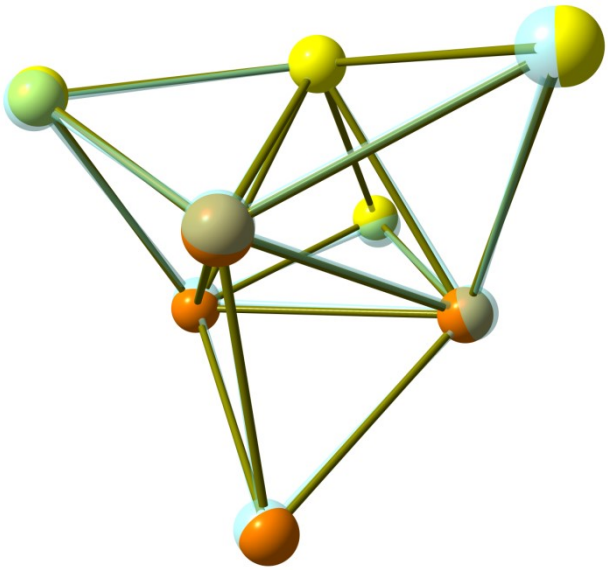

Figure S34. Best superposition of the DFT-optimized Ru_4Au_4 fragments of **5** (orange Ru; yellow Au; white H) with the X-Ray data (transparent cyan).